Check for updates

Daniel C. McFarland
Department of Mechanical and Aerospace Engineering,
North Carolina State University,
911 Oval Drive,
Raleigh, NC 27606
e-mail: dcmcfarl@ncsu.edu

Emily M. McCain
Department of Mechanical and Aerospace Engineering,
North Carolina State University,
911 Oval Drive,
Raleigh, NC 27606
e-mail: emmccain@ncsu.edu

Michael N. Poppo
Department of Mechanical and Aerospace Engineering,
North Carolina State University,
911 Oval Drive,
Raleigh, NC 27606
e-mail: mnpoppo@ncsu.edu

Katherine R. Saul[1]
Department of Mechanical and Aerospace Engineering,
North Carolina State University,
911 Oval Drive,
Raleigh, NC 27606
e-mail: ksaul@ncsu.edu

Spatial Dependency of Glenohumeral Joint Stability During Dynamic Unimanual and Bimanual Pushing and Pulling

Degenerative wear to the glenoid from repetitive loading can reduce effective concavity depth and lead to future instability. Workspace design should consider glenohumeral stability to prevent initial wear. While glenohumeral stability has been previously explored for activities of daily living including push–pull tasks, whether stability is spatially dependent is unexplored. We simulated bimanual and unimanual push–pull tasks to four horizontal targets (planes of elevation: 0 deg, 45 deg, 90 deg, and 135 deg) at 90 deg thoracohumeral elevation and three elevation targets (thoracohumeral elevations: 20 deg, 90 deg, 170 deg) at 90 deg plane of elevation. The 45 deg horizontal target was most stable regardless of exertion type and would be the ideal target placement when considering stability. This target is likely more stable because the applied load acts perpendicular to the glenoid, limiting shear force production. The 135 deg horizontal target was particularly unstable for unimanual pushing (143% less stable than the 45 deg target), and the applied force for this task acts parallel to the glenoid, likely creating shear forces or limiting compressive forces. Pushing was less stable than pulling (all targets except sagittal 170 deg for both task types and horizontal 45 deg for bimanual) ($p < 0.01$), which is consistent with prior reports. For example, unimanual pushing at the 90 deg horizontal target was 197% less stable than unimanual pulling. There were limited stability benefits to task placement for pushing, and larger stability benefits may be seen from converting tasks from push to pull rather than optimizing task layout. There was no difference in stability between bimanual and unimanual tasks, suggesting no stability benefit to bimanual operation. [DOI: 10.1115/1.4043035]

Downloaded from https://asmedigitalcollection.asme.org/biomechanical/article-pdf/141/5/051006/6389652/bio_141_05_051006.pdf by Northwestern University user on 22 June 2020

Introduction

The glenohumeral joint is the most mobile joint in the human body due to a lack of an intrinsically stable osseous socket, like that of hip joint acetabulum. As a result, this joint relies on a combined effort of passive structures and active contributions of muscles, with muscles acting as the primary stabilizers during motion. Damage to these active and passive structures can limit the ability to stabilize the glenohumeral joint [1–4], and reduction in stability is often linked to prior episodes of instability [5]. For example, Marchi et al. [5] reported a reduction in stability index, a measure of computed shear to compressive forces, for subjects with prior dislocation when compared against healthy controls. Furthermore, atraumatic instability [3,6] and/or degenerative wear to the glenoid concavity from repetitive loading can compromise the glenoid concavity. Lippitt and Matsen [4] performed a cadaveric study on glenohumeral stability and reported reductions in stability after resection of the labrum. Their study concluded that any wear or damage that reduces the depth of this concavity would result in a reduction to stability. Active stabilization from muscles is provided through concavity compression, compressing the humeral head into the glenoid cavity, and scapulohumeral balance, balancing the net joint reaction force through the glenoid fossa [4]. Therefore, joint reaction forces composed of large ratios of shear to compressive forces destabilize the joint and pose greater risk for shoulder instability and joint degeneration.

To prevent initial damage to these joint structures, workspace design should consider glenohumeral joint reaction force to avoid motions that naturally place the shoulder at higher risk for instability. Pushing and pulling are frequently performed occupational tasks [7,8], and while muscular demand during isometric [9] and dynamic [10] push–pull tasks have been shown to be spatially dependent, whether this spatial dependency extends to stability is unclear. Furthermore, unimanual and bimanual operation during dynamic pushing and pulling result in differing muscle demands [10], and these differences may also apply to joint stability. Previous studies have reported differences in stability between pushing and pulling [5] but not as a function of task location. Pushing results in unstable joint reaction forces for both cart pushing [11] and hand positioning tasks [5], whereas pulling results in stable joint reaction forces during a functional pull from in front of the body [12] and hand positioning tasks [5]. The stability index during activities of daily living [13] has been shown to depend on shoulder posture, but this index has not been used to evaluate workspace layout. Knowledge of whether these risks are spatially dependent with task target, i.e., hand location at the end of the task, is necessary to inform safer workspace design that incurs less wear to the glenohumeral joint.

This research aims to expand understanding of how task design affects glenohumeral joint instability, and whether smarter workspace design can reduce loading associated with risks for degenerative wear and subsequent instability issues. The objective of this study was to evaluate how task target and task type (unimanual and bimanual pushing and pulling) influence stability at the glenohumeral joint. Our hypotheses for this study were that (i) task target would influence the ratio of shear to compressive forces acting at the shoulder and (ii) pushing would result in larger ratios of shear to compressive forces than pulling. Since the modern industrial workspace is typically characterized by light repetitive work [14], submaximal loading was evaluated.

[1]Corresponding author.
Manuscript received July 31, 2018; final manuscript received February 18, 2019; published online March 25, 2019. Assoc. Editor: Steven D. Abramowitch.

 Copyright © 2019 by ASME

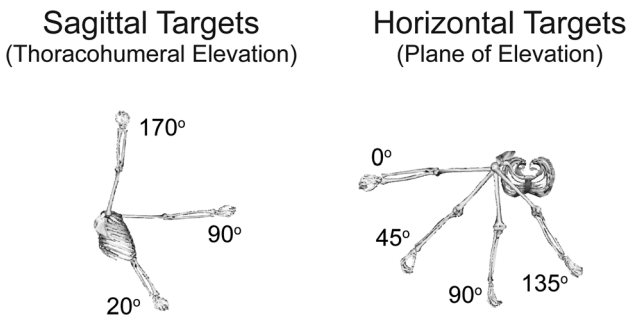

Fig. 1 Task targets. Unimanual and bimanual push and pull simulations were performed for four horizontal targets defined by the plane of elevation angle achieved at the target (0 deg, 45 deg, 90 deg, and 135 deg) at thoracohumeral elevation of 90 deg and three sagittal targets defined by the thoracohumeral elevation angle achieved at the target (20 deg, 90 deg, 170 deg) at plane of elevation of 90 deg, for a total of six independent task targets. Bimanual tasks to the lateral 0 deg horizontal target were not simulated due to the extremely restricted handle motion and joint rotations observed.

Methods

Experimental Protocol. Experimental data were previously recorded from 14 healthy young adults (6 males/8 females) 20 to 32 years old while performing unimanual and bimanual push–pull tasks [10]; these data informed the computational simulations evaluated here. The participants had the following inclusion criteria: (1) no history of upper limb injury or pathology, (2) no neuromuscular impairments, and (3) no physical impediments to performing the required exertions. All subjects were self-reported right-dominant, and the right hand was used for all unimanual tasks. All subjects provided written informed consent in accordance with North Carolina State University Institutional Review Board. A brief summary of the pertinent experimental data collected in the previous study is provided here, as well as a summary of additional data obtained at the time of data collection but not previously reported.

Maximum isometric joint moments for shoulder abduction and elbow flexion of the dominant arm were collected (Biodex System 4 Quick Set, Biodex, Shirley, NY) following a previously described standard protocol [15]. Maximum isometric shoulder abduction moment was assessed with the shoulder abducted to 60 deg and the elbow braced in full extension. Maximum isometric elbow flexion moment was assessed with the shoulder in neutral abduction and the elbow flexed to 90 deg. Three trials of each exertion were obtained; participants received standardized verbal and visual feedback to encourage maximum isometric moments. The maximum moment was determined as the peak isometric moment of the three trials sustained for at least 0.5 s. To minimize fatigue, 60 s of rest were provided between trials.

A series of submaximal unimanual and bimanual push and pull tasks were performed by subjects on a custom pulley system [10]. Loading for all tasks was 15% of subject maximum push–pull capacity measured with the arm in 90 deg forward flexion determined with a closed-chain Biodex attachment using the same protocol as for the isometric joint moments. Loading of 15% maximal capacity was applied with weights to the custom pulley system to the nearest 0.25 lbs. Tasks were performed to targets located at four horizontal positions, defined by the plane of elevation angle achieved at the target (0 deg, 45 deg, 90 deg, and 135 deg) at 90 deg thoracohumeral elevation and three sagittal positions, defined by the thoracohumeral elevation angle achieved at the target (20 deg, 90 deg, 170 deg) at 90 deg plane of elevation, for a total of six independent task targets (Fig. 1). The custom device has a resistance pulley system employing a linear track that allows for height adjustment and locks at three angles to achieve the thoracohumeral elevation angle targets. Plane of elevation targets were achieved by rotating the seat. Bimanual pushes and pulls to the lateral 0 deg horizontal target resulted in

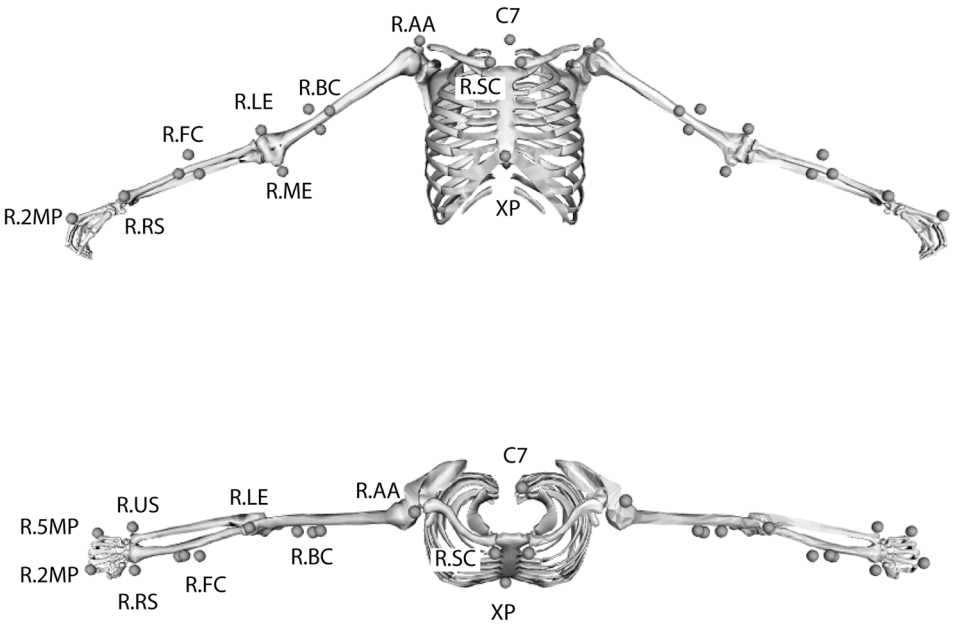

Fig. 2 Upper limb marker set. Retro-reflective motion capture markers (gray spheres) were placed on anatomical locations. Only the right side (denoted by R.) and neutral markers are labeled in the figure; left markers are mirrored from right side. Markers include the seventh cervical vertebra (C7), the most ventral aspect of the sternoclavicular joint (SC), xiphoid process (XP), the most lateral aspect of the acromial angle (AA), a biceps cluster of three markers (BC), the lateral epicondyle of the humerus (LE), the medial epicondyle of the humerus (ME), a forearm cluster of three markers (FC), the styloid process of the radius (RS), the styloid process of the ulna (US), the second metacarpophalangeal joint (2MP), and the fifth metacarpophalangeal joint (5MP).

Downloaded from https://asmedigitalcollection.asme.org/biomechanical/article-pdf/141/5/051006/6389652/bio_141_05_051006.pdf by Northwestern University user on 22 June 2020

Table 1 Removed simulated

Task type	Task target	Subject	Reason
Unimanual pull	Horizontal 0 deg	F7	Optimization did not converge
Unimanual push	Sagittal 20 deg	M4	Plane of elevation tracking error of 16.2 deg
Unimanual pull	Sagittal 20 deg	M5	Plane of elevation tracking error of 10.9 deg
Bimanual push	Sagittal 20 deg	F1	Optimization did not converge
Bimanual pull	Sagittal 20 deg	F2	Optimization did not converge
Bimanual push	Horizontal 45 deg	F2	Optimization did not converge
Bimanual pull	Horizontal 45 deg	F2	Optimization did not converge
Bimanual push	Sagittal 170 deg	F2	Optimization did not converge
Bimanual push	Sagittal 20 deg	F4	Optimization did not converge
Bimanual pull	Sagittal 20 deg	F4	Plane of elevation tracking error of 7.1 deg
Bimanual push	Sagittal 20 deg	F7	Plane of elevation tracking error of 9.1 deg
Bimanual pull	Horizontal 135 deg	M2	Optimization did not converge
Bimanual pull	Sagittal 20 deg	M4	Optimization did not converge

extremely restricted range of motion and were, therefore, not simulated. This resulted in a total of 22 unique simulated tasks for each subject.

Bilateral surface electromyographic (EMG) recordings of the anterior, middle, and posterior deltoid, biceps brachii, lateral head of triceps brachii, latissimus dorsi, and pectoralis major were collected during the testing protocol. Recordings were made at 2000 Hz using 1 cm Ag/AgCl dual electrodes with 16-channel capacity (Noraxon Telemyo DTS system, Noraxon, Scottsdale, AZ). Electrodes were placed on the skin overlying the muscle belly following recommendations of Cram and Criswell [16]. EMG recordings were normalized to maximal voluntary contractions obtained during the isometric moment-generating capacity tests [10]. Kinematics data were simultaneously collected at 200 Hz using 7 Hawk and 4 Kestral cameras (Motion Analysis Corporation, Santa Rosa, CA) tracking 1 cm retroreflective markers placed on anatomical landmarks (Fig. 2) [17]. Data was postprocessed and smoothed with a 6 Hz Butterworth filter (Cortex, Motion Analysis Corporation).

Musculoskeletal Modeling. Simulations of these tasks were performed using a previously developed and validated unimanual upper extremity musculoskeletal model [18] implemented in OPENSIM (v.3.3) [19]. The model was extended to a bimanual model by mirroring joint definitions, muscle paths, and muscle properties to the contralateral side. Shoulder kinematics are defined according to the ISB standard [20], and the shoulder rotation coordinate was expanded to −90 deg to 120 deg to allow full range of motion observed during the experimental testing protocol [12]. Muscle force-generating behavior was represented using the muscle model described by Millard et al. [21] with force–length, force–velocity, and tendon curves described by Binder-Markey and Murray [22] to reflect the force profiles implemented in the nominal model [18]. Tendon compliance for the clavicular component of pectoralis major was neglected to improve simulation stability since this muscle-tendon unit had a small ratio of tendon slack length to optimal muscle fiber length [21]. Ligament models representing the coracohumeral ligament and the superior, middle, inferior portions of the glenohumeral ligament were included, with attachment points approximated from mean insertion and origin data obtained in an anatomical study [23]. Mechanical properties of the ligament models were defined from previous tensile strength studies [24,25].

Individualized models representing the participants were developed by scaling the generic model to subject anthropometry and strength. Models were scaled to participants' anthropometry using static motion capture trials. Peak muscle forces of the muscle actuators were scaled to match experimental strength data of shoulder abduction and elbow flexion. The model's muscles were grouped by the joint of primary action (i.e., shoulder, elbow, wrist) [26], and muscles within a group were scaled together to preserve muscle distribution within a functional group [27–29]. For example, all primary shoulder muscles were scaled to the same scale factor. Muscle force scaling was determined by a custom optimization that minimized the difference between experimentally measured maximum voluntary joint moments and the model's isometric capacity in the corresponding posture. To preserve proportionate muscle strength at joints for which strength data was not available, wrist muscles were scaled to an average of the elbow and shoulder scale factors. Symmetry was assumed, and dominant-side scale factors were applied to the nondominant side.

Computational Simulations. Scaled models were used to obtain joint angle trajectories consistent with observed joint marker positions for each task using inverse kinematics. Resultant kinematics was filtered with a zero-phase filter (MATLAB, The Mathworks, Natick, MA). Experimental task loading was applied as an external force to the model, directed along a vector from the initial hand position to the final position in the plane of the task performance. For unimanual tasks, this force was applied to the hand's center of mass. To allow uneven load distribution during the bimanual tasks, external force was applied to the center of a handle body added to the model, with five degrees-of-freedom (DOF) (rotation about the axis along the handle's length was excluded) linked to each hand's center of mass through point constraints.

Computed muscle control (CMC) [30,31] was used to determine muscle activations required to track the experimental joint kinematics. Briefly, the CMC algorithm incorporates error dynamics to determine joint accelerations required to track experimental kinematics, a static optimization to calculate required muscle activations to produce the desired joint accelerations, and an excitation controller to drive a forward dynamic simulation which creates simulated joint kinematics that feedback into the error dynamics. The EMG recordings were used to inform on/off timing of the respective muscle actuators. When the normalized EMG signal was below 0.1, the muscle was considered off and calculated excitation was limited to 0.1. Otherwise, the muscle was considered on, and calculated excitation was not constrained. To prevent theoretical glenohumeral joint subluxation [32–34], an additional penalty term was included during the optimization to constrain the resultant joint reaction force to fall within experimental limits of joint stability [35]. Halder et al. [35] characterized multidirectional concavity compression stability limits (shear to compressive force ratios) at four levels of shoulder abduction and three force levels; these stability limits were determined through cadaveric studies in which the humeral head was compressed into the glenoid fossa with a known load and the shear force in a given direction was increased until the humeral head dislocated. The average stability limits reported were implemented as the limits for the penalty function. When the resultant joint reaction was beyond these experimental limits, a penalty term proportional to the amount over the limit was applied. Reserve actuators were permitted to provide up to 10 N·m of joint torque to track the kinematics [36].

Downloaded from https://asmedigitalcollection.asme.org/biomechanical/article-pdf/141/5/051006/6389652/bio_141_05_051006.pdf by Northwestern University user on 22 June 2020

Joint reaction forces at the glenohumeral joint were determined using the joint reaction analysis tool in OpenSim. Resultant joint reaction forces were decomposed into components in the transverse plane (i.e., superior/inferior and anterior/posterior forces) and compressive direction (medial forces). Because cadaveric studies of concavity compression report stability limits that depend on transverse orientation [4,35], as related to the depth of the glenoid concavity [4,35], calculated peak ratios of shear to compressive forces were adjusted by the stability limit in the direction of the resulting shear force. The stability index used in this study was

$$\frac{(\text{shear force}/\text{compressive force})}{(\text{empirical stability limit})} * 100 \quad (1)$$

where the empirical stability limit was the ratio of shear to compressive force from Halder et al. [35] that caused dislocation in the direction of the shear force calculated here. Differences between the stability ratio normalized by the empirical stability limit were analyzed across task target and task direction (push and pull) for bimanual and unimanual data sets using a two-way analysis of covariance (ANCOVA) ($\alpha < 0.05$) with sex as a covariate. Differences between the stability ratio normalized by the empirical stability limit were analyzed across exertion type (unimanual versus bimanual) with a one-way ANCOVA ($\alpha < 0.05$) with sex as a covariate. For analysis of exertion type, unimanual data for the lateral 0 deg horizontal target was excluded since bimanual simulations for this task target were not performed. When interactions were not present, they were removed from the model and a Tukey's honest significant difference post hoc test was used to analyze results. If an interaction was present, simple main effect test was performed with a one-way ANCOVA at each factor level using a sequential Bonferroni correction to adjust the α. SAS software (v. 9.4, SAS Institute, Inc., Cary, NC) was used for statistical analyses.

Results

Simulation Performance. Average applied external force was 68.95 ± 22.45 N. When separated by sex, applied external force was 54.21 ± 12.25 N for females and 88.59 ± 17.71 N for males. A total of 4.22% of the simulations were removed from the analysis (1.79% of the unimanual tasks and 7.14% of the bimanual tasks). Simulations were removed when the optimization was unable to converge on a solution within the set convergence criteria or when tracking error between input kinematics and simulated kinematics was greater than 5 deg for shoulder degrees-of-freedoms. Nine of the simulations were removed because the optimization failed, and four of the simulations resulted in tracking error above 5 deg for shoulder degrees-of-freedoms. Removed simulations are reported in Table 1. Mean root-mean-squared error between input kinematics and CMC results for the remaining simulations was less than 1 deg for all degrees-of-freedom. Maximum root-mean-squared reserve torque used was 5.04 N·m for any of the simulated trials. This maximum occurred for the shoulder elevation degree-of-freedom during a unimanual push to the sagittal target of 20 deg.

Stability. Both task direction and task target were main effects for unimanual and bimanual tasks ($p < 0.0001$); however, an interaction between task direction and task target was also present ($p = 0.0003$ for unimanual and $p = 0.0234$ for bimanual). Therefore, the interaction was analyzed with a simple main effects test at each level of the interaction.

In general, unimanual pushing was less stable than unimanual pulling, and responded differently to target location. Unimanual pushing was less stable than unimanual pulling ($p < 0.001$) at all task targets except the most elevated: sagittal 170 deg ($p = 0.0503$). For example, unimanual pushing at the 90 deg horizontal target was 197% less stable than unimanual pulling. For unimanual pulling, glenohumeral stability was most sensitive to sagittal target placement. The sagittal targets of 20 deg (low) and 170 deg (high) were significantly less stable than the horizontal targets at 90 deg and 45 deg ($p < 0.001$) (Fig. 3). Pulling to the sagittal 20 deg (low) and 170 deg (high) was 180% and 169% less stable, respectively, than the horizontal 45 deg target. Furthermore, the lateral 0 deg target tended to be less stable than the horizontal 45 deg target ($p = 0.048$), but this was not significant following sequential Bonferroni adjustment. For unimanual pushing, however, horizontal target placement had the largest impact. The cross-body 135 deg horizontal target was significantly less stable than the forward 90 deg and the lateral 45 deg horizontal targets (123% and 143% less stable than the 90 deg and the 45 deg, respectively) ($p = 0.0095$ and $p < 0.0001$, respectively) and the elevated sagittal target of 170 deg ($p = 0.0003$) (Fig. 3). Additionally, for pushing, the lateral 0 deg horizontal target and the sagittal 20 deg target were less stable than the lateral 45 deg horizontal target ($p = 0.0058$ and $p = 0.0133$, respectively). However, for unimanual pushing all mean peak stability indexes were near experimental limits of stability determined through concavity compression [35].

For the dominant limb during bimanual tasks, pushing, in general, was again less stable than pulling, but both bimanual task types had similar response to target location. Bimanual pushing was significantly less stable than bimanual pulling at all targets ($p < 0.01$) except for horizontal 45 deg ($p = 0.289$) and sagittal 170 deg ($p = 0.1947$) (Fig. 4). For example, bimanual pushing at the 90 deg horizontal target was 157% less stable than bimanual pulling. For bimanual pulling, the sagittal targets (20 deg and 170 deg) and the cross-body 135 deg horizontal target were significantly less stable than the lateral 45 deg horizontal target ($p < 0.0001$). Bimanual pulling to the sagittal targets 20 deg and 170 deg targets were 164% and 160% less stable than the 45 deg target, respectively, and the cross-body 135 deg target was 164%

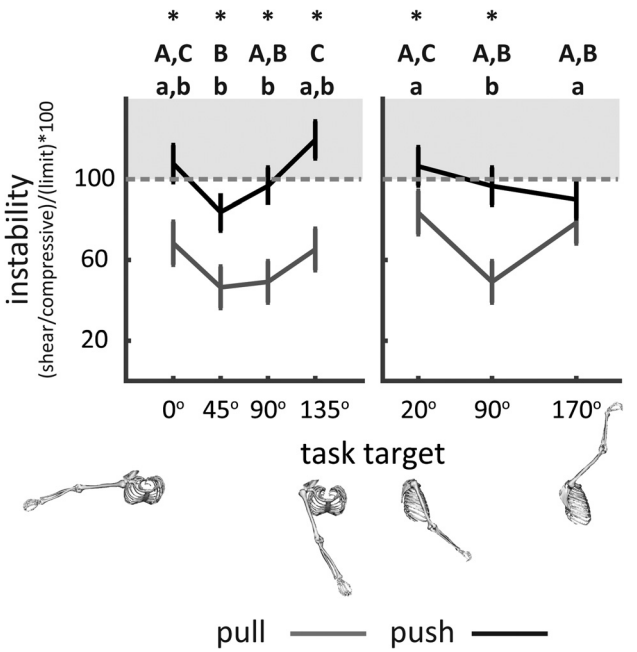

Fig. 3 Unimanual task direction by task target interaction. In general, pushing was less stable than pulling, and had a different spatial dependency from pulling. Unimanual pushing was less stable than unimanual pulling (indicated by *) ($p < 0.001$) at all task targets except the most elevated: sagittal 170 deg ($p = 0.0503$). For pushing, targets with different capital letters are significantly different. For pulling, targets with different lowercase letters are significantly different. Error bars represent 95% confidence interval for adjusted means.

Downloaded from https://asmedigitalcollection.asme.org/biomechanical/article-pdf/141/5/051006/6389652/bio_141_05_051006.pdf by Northwestern University user on 22 June 2020

less stable than the 45 deg target. Bimanual pushing showed a similar response with all other targets being significantly less stable than the lateral 45 deg horizontal target ($p < 0.001$). The least stable 135 deg was 180% less stable than the most stable 45 deg target. However, for bimanual pushing, peak stability indexes for all targets except horizontal 45 deg target were near the experimental limits of stability. Comparison between unimanual and bimanual tasks revealed no difference in stability at the glenohumeral joint ($p = 0.5836$).

Discussion

This work demonstrated that glenohumeral stability during both pushing and pulling was spatially dependent, with the lateral 45 deg horizontal target favoring stability most across exertion types. In general, pushing was less stable than pulling for both unimanual and bimanual tasks. We detected no difference in stability between bimanual and unimanual tasks, suggesting that there may be no stability benefit to bimanual operation at low loading.

For unimanual pulling, sagittal target location had the biggest impact on glenohumeral stability, with the low- and high-sagittal targets being significantly less stable than horizontal targets (specifically, 90 deg and 45 deg). Other researchers have reported that shear loading depends on shoulder elevation for other types of tasks as well [13,37]. For example, Blache et al. [37] evaluated glenohumeral reaction forces during an experimentally driven simulation of a sagittal lifting task from hip level to shoulder level. They reported increased shear force at the beginning and final phase of the motion. Furthermore, they ran their simulations with and without a joint stability constraint [33], and found that shear/compressive forces were near empirical limits when constrained and well over these limits when unconstrained.

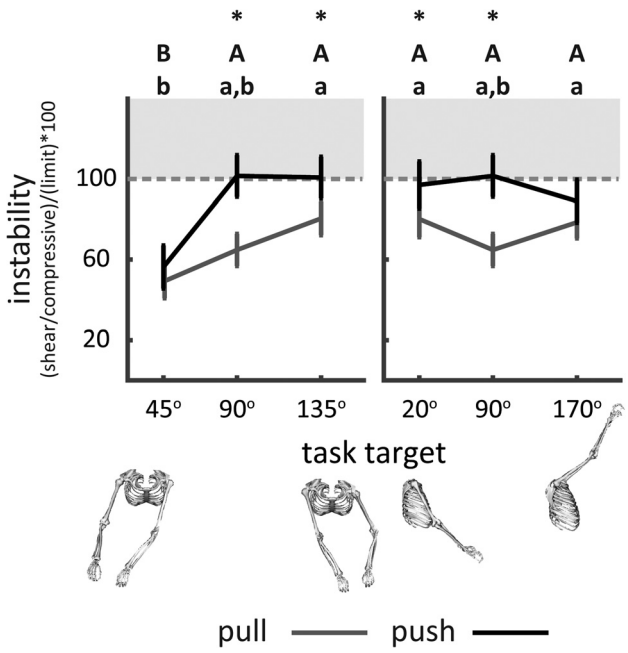

Fig. 4 Bimanual task direction by task target interaction. For bimanual tasks when considering only the dominant shoulder, pushing, in general, was again less stable than pulling, but both bimanual task types had similar response to spatial location of tasks. Bimanual pushing was significantly less stable than bimanual pulling at all targets (indicated by *) ($p < 0.01$) except for horizontal 45 deg ($p = 0.3059$) and sagittal 170 deg ($p = 0.1947$). For pushing, targets with different capital letters are significantly different. For pulling, targets with different lowercase letters are significantly different. Error bars represent 95% confidence interval for adjusted means.

Additionally, Klemt et al. [13] found that reaching to head height with a 0.5 kg weight was less stable than reaching forward with the same weight, similar to the decreased stability we observed for the high target. In the current study, there was no significant dependence for unimanual pulling on horizontal target location, although the most lateral target (0 deg) tended to be less stable than the 45 deg target. The lack of statistical difference may be due to statistical power, since lateral targets during unimanual pulling had wide variability in stability ratios. For unimanual pushing, the cross-body horizontal target of 135 deg was the least stable target, and the applied force direction at the hand is essentially parallel to the glenoid fossa for this task. Therefore, force production for this task target likely results in decreased compressive forces and/or increased shear forces along the anterior–posterior plane of the glenoid fossa contributing to instability. Furthermore, cross-body motion is at the end-range of motion of the glenohumeral joint, where capsular ligaments contribute to stabilization [38,39]. While anterior glenohumeral ligaments and the coracohumeral ligament were modeled here, anterior glenohumeral ligaments are only engaged when the shoulder is in extension or external rotation [39]. Cross-body tasks, however, involve flexion and internal rotation where the posterior capsule, not modeled in this study, undergoes tension [39]. Including the posterior capsule in future modeling may increase predicted stability of this task target, but the results of this study suggest that the muscles do have a limited ability to stabilize the reaction for cross-body tasks. In addition to the instability of the cross-body target, the other extreme posture—lateral 0 deg horizontal target—was significantly less stable than the 45 deg horizontal target for unimanual pushing. This is consistent with the work of Klemt et al. [13], who found that the least stable reaction of all the activities of daily living tested in their study was for a task where subjects moved the limb between a lateral target and a target across the body in the transverse plane. In contrast to targets at the horizontal extremes, the applied force direction for the horizontal 45 deg target is essentially perpendicular to the glenoid; therefore, force production for pushing to this target likely results in a natural increase in compressive reaction forces, thereby making this target particularly stable. Similarly, for both bimanual pushing and pulling, the 45 deg horizontal target was again the most stable task target. Furthermore, there was no difference in stability for bimanual pushing or pulling at this target, suggesting that this target is stable regardless of exertion direction. This increased stability was present for both unimanual and bimanual pushing and pulling, making it the ideal target location when considering glenohumeral stability alone. This task target is in midrange of glenohumeral motion; therefore, stability is provided through active contributions of muscles. Interestingly, a prior study of muscle demand during dynamic pushing and pulling in the same cohort of participants [10] reported that this 45 deg horizontal target was also less demanding than other horizontal targets, as determined from muscle activation. Inherent task stability of this particular target may contribute to the reduced muscle demand. Additional research is needed to fully understand to what degree inherent task stability and required muscled demand are linked.

Prior studies have reported that pushing results in unstable reactions at the glenohumeral joint [5,11], whereas pulling results in more stable reactions [5,12]. In general, the results from this current study agree with these previous studies, with reactions for pushing resulting in less stable reactions for most targets. Of these previous studies, only Marchi et al. [5] directly compared pushing and pulling, considering targets placed directly in front of the subject. Therefore, their results would be most analogous to our results for the horizontal 90 deg target, for which pushing was significantly less stable. Another study by Klemt et al. [13] compared glenohumeral stability during reaching tasks toward and away from the body while holding a thin wooden rod without applied resistance. They report that both these tasks had high shear to compressive force ratios directed inferiorly on the glenoid,

Downloaded from https://asmedigitalcollection.asme.org/biomechanical/article-pdf/141/5/051006/6389652/bio_141_05_051006.pdf by Northwestern University user on 22 June 2020

although the ratio for tasks toward the body were slightly lower than for away. Reported force ratios were above the empirical stability limits reported in Halder et al. [35] for the inferior direction. In our study, pulling at the horizontal 90 deg target resulted in net joint reactions that were within experimental stability limits. This difference in reported stability for pulling is likely related to the difference in applied load between the study by Klemt et al. [13] and ours due to the increased muscle forces needed to resist the applied load. We did not observe a difference between pushing and pulling for the high sagittal target or 45 deg horizontal target for bimanual tasks; no other study has compared glenohumeral stability for these particular task targets. The lack of difference between pushing and pulling at these targets may be partially related to statistical power (difference in pushing and pulling approached significance for unimanual tasks at the sagittal 170 deg target $p = 0.0503$) or related to inherent stability of the joint when forces are directed perpendicularly to the glenoid, as in the 45 deg horizontal target. Since pushing was in general less stable than pulling, designing for stability may see greater benefits from appropriately choosing exertion direction to be a pull rather than attempting to optimize push layout.

Pushing often resulted in stability ratios that were near experimental limits reported by Halder et al. [35]. Subjects in the experimental study, however, did not report pain or instability during the experimental protocol. The experimental limits reported by Halder et al. [35] were determined through cadaveric studies at low compression loads and may be lower than in vivo stability limits at higher compression. Furthermore, concavity compression ratios do depend on posture [35], but are typically measured in an abducted posture [35,40]. Our push and pull tasks required postures that differ from abducted postures, and stability limits in these postures may therefore differ from the experimental limits determined in abduction. Some translation of the humeral head, however, does occur naturally in vivo. During abduction under anterior loading, humeral head translation in vivo is on the order of millimeters [41]. Therefore, it is possible that our testing protocol did result in high shear forces that caused translation of the humeral head within the glenoid fossa.

Bimanual operation did not result in a significant increase in stability, suggesting that there may be limited stability benefit from switching to bimanual operation at low loading. Stability benefits of bimanual operation, however, may exist if loading is increased. Previous work has shown that reducing the applied load reduces the demand on shoulder muscles for isometric tasks [42] and that bimanual operation reduced demand on the dominant shoulder for dynamic push–pull tasks [10]. While glenohumeral stability is related to this combined muscular effort balancing the net joint reaction, this reduction in demand does not appear to be associated with overall stability.

Study limitations should be taken into consideration when interpreting these results. Subject history of upper limb injury was self-reported, and subjects were not screened for presence of an asymptomatic injury. Shoulder injury, such as a rotator cuff tear, can alter kinematic choices and EMG signaling [43], which could affect joint loading and stability ratios. These injuries, however, are primarily present in older adults [44], and our population was young healthy adults. Although subjects received instructions regarding approximate trial timing, task speed was not explicitly controlled. However, workers typically perform tasks at a self-selected speed and thus this approach may be more representative of industrial settings. Subjects performed tasks in a seated posture with their torso restrained to isolate the effects of task on shoulder kinematics. However, in an industrial setting, workers are typically unconstrained and may rely more heavily on torso rotation to complete tasks. Incorporating torso rotation into the movement strategy would require less shoulder motion to reach the lateral horizontal targets; therefore, the range of shoulder motion in an industrial setting may be less extreme than the targets evaluated in this study. Strength scaling was limited to measurements collected for shoulder abduction and elbow flexion in one posture each, and subjects' strength profile in other postures and for other joints was assumed to follow the same relative profile as the default model. Individual strength profiles across postures can vary [45,46]. Strength of individual muscles was scaled with their primary joint of action since muscle volume distribution is highly conserved across adults [27–29]. If muscle volume distribution in these subjects differed from reported values in the literature, then individual muscle forces would vary correspondingly; however, we did not have imaging data available to evaluate this. Furthermore, strength data of the nondominant arm and the wrist of the dominant arm were not collected, so strength symmetry was assumed. Finally, in the simulations the applied force was limited to planar directions to correspond to the controlled handle loading and motion in the experiment along a linear track; however, in the experimental study there may have been limited nonplanar components of the applied force as well.

Conclusion

While glenohumeral stability has been previously explored for push–pull tasks, whether stability is dependent on the spatial location of the task has been previously unexplored. We found the glenohumeral joint reaction was most stable for all task types (unimanual and bimanual pushing and pulling) when the applied force was directed essentially perpendicular to the glenoid, thereby limiting shear force production. Therefore, placing push–pull tasks near this task target may improve inherent joint stability, which may ultimately help reduce degenerative wear to the glenoid. Pushing, in general, was less stable than pulling and had predicted stability ratios nearing empirical stability limits, suggesting that stability benefits may be seen from converting tasks from push to pull tasks. Finally, there was no difference in stability between bimanual and unimanual tasks, suggesting limited stability benefit to bimanual operation at low loading.

Acknowledgment

We would like to thank Alexander Brynildsen and Lauren Levine for their assistance in postprocessing kinematic data.

Funding Data

- CFD Research Corporation.

References

[1] Steenbrink, F., de Groot, J. H., Veeger, H. E. J., van der Helm, F. C. T., and Rozing, P. M., 2009, "Glenohumeral Stability in Simulated Rotator Cuff Tears," J. Mech., **42**(11), pp. 1740–1745.

[2] van Drongelen, S., Schlüssel, M., Arnet, U., and Veeger, D., 2013, "The Influence of Simulated Rotator Cuff Tears on the Risk for Impingement in Handbike and Handrim Wheelchair Propulsion," Clin. Mech., **28**(5), pp. 495–501.

[3] Lazarus, M. D., Sidles, J. A., Harryman, D. T., and Matsen, F. A., II, 1996, "Effect of a Chondral-Labral Defect on Glenoid Concavity and Glenohumeral Stability. A Cadaveric Model," J. Bone Jt. Surg., **78**(1), pp. 94–102.

[4] Lippitt, S. B., and Matsen, F., 1993, "Mechanisms of Glenohumeral Joint Stability," Clin. Orthop. Relat. Res., **291**, pp. 20–28.

[5] Marchi, J., Blana, D., and Chadwick, E. K., 2014, "Glenohumeral Stability During a Hand-Positioning Task in Previously Injured Shoulders," Med. Biol. Eng. Comput., **52**(3), pp. 251–256.

[6] Rowe, C. R., Patel, D., and Southmayd, W. W., 1978, "The Bankart Procedure: A Long-Term End-Result Study," J. Bone Jt. Surg., **60**(1), pp. 1–16.

[7] Lind, C. M., 2018, "Pushing and Pulling: An Assessment Tool for Occupational Health and Safety Practitioners," Int. J. Occup. Saf. Ergon., **24**(1), pp. 14–26.

[8] Baril-Gingras, G., and Lortie, M., 1995, "The Handling of Objects Other Than Boxes: Univariate Analysis of Handling Techniques in a Large Transport Company," Ergonomics, **38**(5), pp. 905–925.

[9] McDonald, A., Picco, B. R., Belbeck, A. L., Chow, A. Y., and Dickerson, C. R., 2012, "Spatial Dependency of Shoulder Muscle Demands in Horizontal Pushing and Pulling," Appl. Ergon., **43**(6), pp. 971–978.

[10] McFarland, D. C., Poppo, M. N., McCain, E. M., and Saul, K. R., 2018, "Spatial Dependency of Shoulder Muscle Demand During Dynamic Unimanual and Bimanual Pushing and Pulling," Appl. Ergon., **73**, pp. 199–205.

[11] Nimbarte, A. D., Sun, Y., Jaridi, M., and Hsiao, H., 2013, "Biomechanical Loading of the Shoulder Complex and Lumbosacral Joints During Dynamic Cart Pushing Task," Appl. Ergon., **44**(5), pp. 841–849.

Downloaded from https://asmedigitalcollection.asme.org/biomechanical/article-pdf/141/5/051006/6389652/bio_141_05_051006.pdf by Northwestern University user on 22 June 2020

[12] Vidt, M. E., Santago, A. C., Marsh, A. P., Hegedus, E. J., Tuohy, C. J., Poehling, G. G., Freehill, M. T., Miller, M. E., and Saul, K. R., 2018, "Modeling a Rotator Cuff Tear: Individualized Shoulder Muscle Forces Influence Glenohumeral Joint Contact Force Predictions," Clin. Mech., **60**, pp. 20–29.
[13] Klemt, C., Prinold, J. A., Morgans, S., Smith, S. H. L., Nolte, D., Reilly, P., and Bull, A. M. J., 2018, "Analysis of Shoulder Compressive and Shear Forces During Functional Activities of Daily Life," Clin. Mech., **54**, pp. 34–41.
[14] Das, B., and Sengupta, A. K., 1996, "Industrial Workstation Design: A Systematic Ergonomics Approach," Appl. Ergon., **27**(3), pp. 157–163.
[15] Holzbaur, K. R. S., Delp, S. L., Gold, G. E., and Murray, W. M., 2007, "Moment-Generating Capacity of Upper Limb Muscles in Healthy Adults," J. Mech., **40**(11), pp. 2442–2449.
[16] Cram, J. R., and Criswell, E., 2011, *Cram's Introduction to Surface Electromyography*, Jones and Bartlett, Sudbury, MA.
[17] Vidt, M. E., Santago, A. C., Marsh, A. P., Hegedus, E. J., Tuohy, C. J., Poehling, G. G., Freehill, M. T., Miller, M. E., and Saul, K. R., 2016, "The Effects of a Rotator Cuff Tear on Activities of Daily Living in Older Adults: A Kinematic Analysis," J. Mech., **49**(4), pp. 611–617.
[18] Saul, K. R., Hu, X., Goehler, C. M., Vidt, M. E., Daly, M., Velisar, A., and Murray, W. M., 2015, "Benchmarking of Dynamic Simulation Predictions in Two Software Platforms Using an Upper Limb Musculoskeletal Model," Comput. Methods Mech. Biomed. Eng., **18**(13), pp. 1445–1458.
[19] Delp, S. L., Anderson, F. C., Arnold, A. S., Loan, P., Habib, A., John, C. T., Guendelman, E., and Thelen, D. G., 2007, "OpenSim: Open-Source Software to Create and Analyze Dynamic Simulations of Movement," IEEE Trans. Biomed. Eng., **54**(11), pp. 1940–1950.
[20] Wu, G., van der Helm, F. C. T., (DirkJan) Veeger, H. E. J., Makhsous, M., Van Roy, P., Anglin, C., Nagels, J., Karduna, A. R., McQuade, K., Wang, X., Werner, F. W., and Buchholz, B., 2005, "ISB Recommendation on Definitions of Joint Coordinate Systems of Various Joints for the Reporting of Human Joint Motion—Part II: Shoulder, Elbow, Wrist and Hand," J. Mech., **38**(5), pp. 981–992.
[21] Millard, M., Uchida, T., Seth, A., and Delp, S. L., 2013, "Flexing Computational Muscle: Modeling and Simulation of Musculotendon Dynamics," ASME J. Biomech. Eng., **135**(2), p. 021005.
[22] Binder-Markey, B. I., and Murray, W. M., 2017, "Incorporating the Length-Dependent Passive-Force Generating Muscle Properties of the Extrinsic Finger Muscles Into a Wrist and Finger Biomechanical Musculoskeletal Model," J. Mech., **61**, pp. 250–257.
[23] Yang, C., Goto, A., Sahara, W., Yoshikawa, H., and Sugamoto, K., 2010, "In Vivo Three-Dimensional Evaluation of the Functional Length of Glenohumeral Ligaments," Clin. Mech., **25**(2), pp. 137–141.
[24] Boardman, N. D., Debski, R. E., Warner, J. J. P., Taskiran, E., Maddox, L., Imhoff, A. B., Fu, F. H., and Woo, S. L.-Y., 1996, "Tensile Properties of the Superior Glenohumeral and Coracohumeral Ligaments," J. Shoulder Elbow Surg., **5**(4), pp. 249–254.
[25] Bigliani, L. U., Pollock, R. G., Soslowsky, L. J., Flatow, E. L., Pawluk, R. J., and Mow, V. C., 1992, "Tensile Properties of the Inferior Glenohumeral Ligament," J. Orthop. Res., **10**(2), pp. 187–197.
[26] Daly, M., Vidt, M. E., Eggebeen, J. D., Simpson, W. G., Miller, M. E., Marsh, A. P., and Saul, K. R., 2013, "Upper Extremity Muscle Volumes and Functional Strength After Resistance Training in Older Adults," J. Aging Phys. Act., **21**(2), pp. 186–207.
[27] Holzbaur, K. R. S., Murray, W. M., Gold, G. E., and Delp, S. L., 2007, "Upper Limb Muscle Volumes in Adult Subjects," J. Mech., **40**(4), pp. 742–749.
[28] Saul, K. R., Vidt, M. E., Gold, G. E., and Murray, W. M., 2015, "Upper Limb Strength and Muscle Volume in Healthy Middle-Aged Adults," ASME J. Appl. Mech., **31**(6), pp. 484–491.
[29] Vidt, M. E., Daly, M., Miller, M. E., Davis, C. C., Marsh, A. P., and Saul, K. R., 2012, "Characterizing Upper Limb Muscle Volume and Strength in Older Adults: A Comparison With Young Adults," J. Mech., **45**(2), pp. 334–341.
[30] Thelen, D. G., Anderson, F. C., and Delp, S. L., 2003, "Generating Dynamic Simulations of Movement Using Computed Muscle Control," J. Mech., **36**(3), pp. 321–328.
[31] Thelen, D. G., and Anderson, F. C., 2006, "Using Computed Muscle Control to Generate Forward Dynamic Simulations of Human Walking From Experimental Data," J. Mech., **39**(6), pp. 1107–1115.
[32] Chadwick, E. K., Blana, D., van den Bogert, A. J. T., and Kirsch, R. F., 2009, "A Real-Time, 3-D Musculoskeletal Model for Dynamic Simulation of Arm Movements," IEEE Trans. Bio-Med. Eng., **56**(4), pp. 941–948.
[33] Dickerson, C. R., Chaffin, D. B., and Hughes, R. E., 2007, "A Mathematical Musculoskeletal Shoulder Model for Proactive Ergonomic Analysis," Comput. Methods Mech. Biomed. Eng., **10**(6), pp. 389–400.
[34] van der Helm, F., 1994, "A Finite Element Musculoskeletal Model of the Shoulder Mechanism," J. Mech., **27**(5), pp. 551–569.
[35] Halder, A. M., Kuhl, S. G., and Zobitz, M. E., 2001, "Effects of the Glenoid Labrum and Glenohumeral Abduction on Stability of the Shoulder Joint Through Concavity-Compression: An In Vivo Study," J. Bone Jt. Surg., **83-A**(7), pp. 1062–1069.
[36] Hicks, J. L., Uchida, T. K., Seth, A., Rajagopal, A., and Delp, S. L., 2015, "Is My Model Good Enough? Best Practices for Verification and Validation of Musculoskeletal Models and Simulations of Movement," ASME J. Biomech. Eng., **137**(2), p. 020905.
[37] Blache, Y., Begon, M., Michaud, B., Desmoulins, L., Allard, P., and Dal Maso, F., 2017, "Muscle Function in Glenohumeral Joint Stability During Lifting Task," PLoS One, **12**(12), p. e0189406.
[38] Harryman, D. T., Sidles, J. A., Clark, J. M., McQuade, K. J., Gibb, T. D., and Matsen, F. A., 1990, "Translation of the Humeral Head on the Glenoid With Passive Glenohumeral Motion," J. Bone Jt. Surg., **72**(9), pp. 1334–1343.
[39] Terry, G. C., Hammon, D., France, P., and Norwood, L. A., 1991, "The Stabilizing Function of Passive Shoulder Restraints," Am. J. Sports Med., **19**(1), pp. 26–34.
[40] Lippitt, S. B., Vanderhooft, J. E., Harris, S. L., Sidles, J. A., Harryman, D. T., and Matsen, F. A., 1993, "Glenohumeral Stability From Concavity-Compression: A Quantitative Analysis," J. Shoulder Elbow Surg., **2**(1), pp. 27–35.
[41] Cereatti, A., Calderone, M., Buckland, D. M., Buettner, A., Della Croce, U., and Rosso, C., 2014, "In Vivo Glenohumeral Translation Under Anterior Loading in an Open-MRI Set-Up," J. Mech., **47**(15), pp. 3771–3775.
[42] Meszaros, K. A., Vidt, M. E., and Dickerson, C. R., 2018, "The Effects of Hand Force Variation on Shoulder Muscle Activation During Submaximal Exertions," Int. J. Occup. Saf. Ergon., **24**(1), pp. 100–110.
[43] Hawkes, D. H., Alizadehkhaiyat, O., Kemp, G. J., Fisher, A. C., Roebuck, M. M., and Frostick, S. P., 2012, "Shoulder Muscle Activation and Coordination in Patients With a Massive Rotator Cuff Tear: An Electromyographic Study," J. Orthop. Res., **30**(7), pp. 1140–1146.
[44] Minagawa, H., Yamamoto, N., Abe, H., Fukuda, M., Seki, N., Kikuchi, K., Kijima, H., and Itoi, E., 2013, "Prevalence of Symptomatic and Asymptomatic Rotator Cuff Tears in the General Population: From Mass-Screening in One Village," J. Orthop., **10**(1), pp. 8–12.
[45] Garner, B. A., and Pandy, M. G., 2001, "Musculoskeletal Model of the Upper Limb Based on the Visible Human Male Dataset," Comput. Methods Mech. Biomed. Eng., **4**(2), pp. 93–126.
[46] Otis, J. C., Warren, R. F., Backus, S. I., Santner, T. J., and Mabrey, J. D., 1990, "Torque Production in the Shoulder of the Normal Young Adult Male. The Interaction of Function, Dominance, Joint Angle, and Angular Velocity," Am. J. Sports Med., **18**(2), pp. 119–123.

Downloaded from https://asmedigitalcollection.asme.org/biomechanical/article-pdf/141/5/051006/6389652/bio_141_05_051006.pdf by Northwestern University user on 22 June 2020